Spatio-temporal variations in hydro-physical and -chemical parameters during a major upwelling event off the southern coast of the Gulf of Finland in summer 2006*

Ülo Suursaar*
Robert Aps

Estonian Marine Institute,
University of Tartu,
Mäealuse 10a, EE–12618 Tallinn, Estonia;

e-mail: ulo.suursaar@ut.ee

*corresponding author

Abstract

The objective of the paper is to document and examine the major upwelling event that occurred along the northern coast of Estonia in August 2006. With a horizontal extension of 360 km, the event was caused by persistent easterlies and was noticed by a large number of holidaymakers, as it reduced the temperature of the coastal sea to a chilly 5–10°C for about a month. *In situ* measurements from an RDCP current profiler revealed an along-wind coastal jet of up to 60 cm s^{-1} and a weak near-bottom countercurrent. The depths of the pycnocline and nutricline rose. The maximum drop in water temperature was 16°C, that of salinity was 3.6 PSU. Analysis of satellite images confirmed the large extension and the prominence of the event.

The complete text of the paper is available at http://www.iopan.gda.pl/oceanologia/

1. Introduction

Along the northern coast of Estonia during early August 2006, a clear upwelling evolved which lasted, together with short recession periods, for over a month. The event was caused by unusually persistent easterlies of a moderate strength and was noticed by a large number of local residents as well as by holidaymakers, as it reduced the nearshore sea surface temperature from the usual summertime 18–21°C to an uncomfortable 5–15°C. The longshore extension of the affected coastline seemed to be at least 200–300 km. The event received quite wide coverage in the Estonian newspapers and mass media, but its evolution and impact on the coastal marine environment has not yet been adequately analysed.

Actually, upwelling is not such a rare event at all. Quasi-permanent large-scale upwellings occur in many coastal areas and current divergence zones of the World Ocean. A pronounced vertical structure of both currents and biological properties can be found in convergence and divergence zones, and near fronts and estuaries (e.g. Bowden 1983, Yanagi et al. 1995). In the Baltic Sea, upwelling is more variable and mainly a mesoscale – synoptic scale process. Several driving mechanisms may be involved, but usually it is produced by a wind blowing alongshore with the coastline on the left-hand side when looking downwind. This time-variable wind-forced upward displacement of water is connected to the offshore drift (also called the Ekman shift) of the flows due to the Coriolis force (e.g. Gill & Clarke 1974, Bowden 1983). For example, in the case of westerly winds, it calls for a compensatory upward flow along the northern coast of the Gulf of Finland, and a downward flow along the southern coast. Owing to the prevailing regional south-westerly and westerly winds, this is a rather frequent situation with an upwelling persistency of up to 30% off the Finnish coast and a 25% downwelling persistency along the Estonian coast (Myrberg & Andrejev 2003). Although there is a clear connection between the predominant climatological wind directions and the corresponding locations of coastal upwelling zones (e.g. Myrberg & Andrejev 2003, Kowalewski & Ostrowski 2005), a certain climatological shift of these zones may occur in the future (e.g. Suursaar & Kullas 2006).

According to the definition, upwelling should be primarily understood as the existence of a vertical component in the flow field. As the real vertical velocities are difficult to measure, several indirect methods are used. Firstly, spatio-temporal variations in water temperature have been used as indicators of upwellings. The effects of upwelling on water temperature, salinity or other substances were originally measured *in situ* (e.g. Walin 1972, Haapala 1994, Lass et al. 1994). More recently, studies based on satellite images have been published (e.g. Gidhagen 1987, Bychkova

& Viktorov 1987, Kręžel et al. 2005a). On a satellite image or *in situ* temperature record, upwelling can only be registered when the temperature of the surface layer differs significantly from that of the deeper waters. This means that upwelling is 'visible' and biologically influential when the isopycnal layers are close to each other and the thermo- and nutriclines are not too deep. Otherwise, excessively large and continuous upflows are required for reaching the surface, and the favourable wind conditions should be very persistent. And finally, upwelling can also be calculated by hydrodynamic 3D models. In the Baltic Sea they include the studies by Lehmann et al. (2002), Jankowski (2002), Myrberg & Andrejev (2003), Kowalewski & Ostrowski (2005).

Because of technical difficulties and the relatively small values to be measured, direct measurements of vertical velocities are rare. Nevertheless, vertical fluxes can also be estimated on the basis of the vertical structure of horizontal currents. Traditionally, current meters have been deployed at certain specific depths within the water column, each depth requiring an individual instrument. Only in recent years has the three-dimensional velocity structure increasingly been investigated by means of instruments using the Doppler effect of acoustic beams. Acoustic Doppler current profilers (ADCPs) and recording Doppler current profilers (RDCPs) have proved very useful in studies of frontal structures and upwelling – initially, mainly in the USA (e.g. Marmorino & Trump 1992, Geyer 1993), but recently also in Europe (e.g. Wewetzer et al. 1999).

The role of vertical fluxes in the coastal marine ecosystem is rather diverse, as large quantities of energy and matter are exchanged between the surface and deep layers by means of vertical flows. The upwelled water is usually rich in nutrients, and coastal upwelling regions are among the most important fishing regions of the World Ocean. In the Baltic Sea, as in many other regions, upwelling triggers profound changes in the phytoplankton community and productivity (Nõmmann et al. 1991, Ennet et al. 2000). However, in shelf seas like the Baltic Sea, the influence of coastal upwelling on the productivity of the surface layer may not be as obvious as in an oceanic event. Some contrasting effects on productivity in the Baltic Sea have been discussed, e.g. by Kręžel et al. (2005b) and Vahtera et al. (2005).

The main objectives of this paper are: (1) to document the scale and evolution of the summer 2006 upwelling event in the Gulf of Finland on the basis of *in situ* oceanographic measurements and satellite images; (2) to examine its driving conditions and hydrodynamic properties, and to study the possible impact of the event on the hydrochemical and hydrobiological conditions of the Gulf of Finland. In addition, we present a short overview

of an oceanographic measuring complex called RDCP-600 and assess our experiences with investigating the vertical structure of currents with that instrument.

2. Material and methods

2.1. Meteorological and hydrological data

The Estonian Meteorological and Hydrological Institute (EMHI) carries out routine meteorological and hydrological observations. For wind forcing, we used data from the Kunda and Pakri meteorological stations (Fig. 1).While Kunda was the station closest to our measurement site, just 10 km away, the southerlies and westerlies blowing there are somewhat influenced by the land shadow. Data from Pakri, 150 km to the west, better describe the winds from the west and can be used as background information for the open part of the Gulf of Finland. The stations are equipped with a MILOS-520 automatic weather complex and provide the hourly average wind speed, gust wind speed and hourly prevailing wind direction.
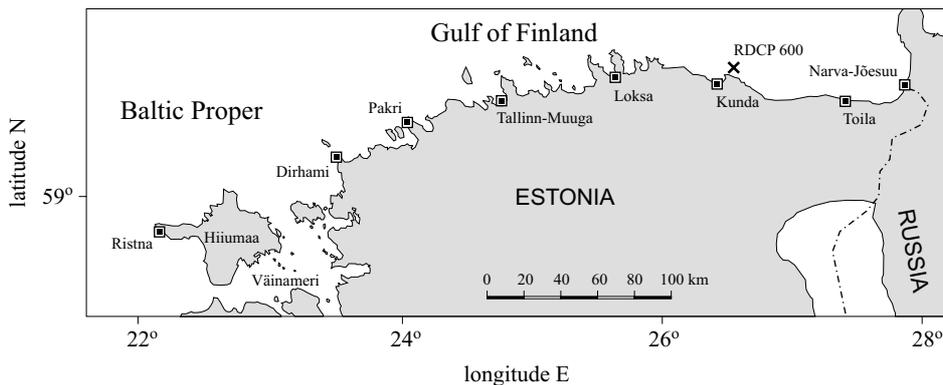
Fig. 1. Map of the study area with the locations of selected stations operated by the Estonian Meteorological and Hydrological Institute, and the RDCP-600 mooring site

Twice daily, the sea surface water temperature is measured at coastal marine stations. We used morning (6 UTC) data, which are less influenced by summertime diurnal variations, from Ristna, Dirhami, Pakri, Loksa, Kunda, Toila and Narva-Jõesuu (Fig. 1), and also sea level data from the Narva Jõesuu tide gauge. The tide gauge, operated by the EMHI, provides hourly data. For comparison with RDCP-600 readings, we calculated daily average sea level values.

2.2. *In situ* measurements

For studying the hydrodynamic regime of the coastal waters near Kunda (Fig. 1), a Recording Doppler Current Profiler RDCP-600 from AADI Aanderaa Instruments was used. The instruments, referred to by different manufacturers as DCM (Doppler current meter), ADCP or RDCP, apply the Doppler effect to measure velocity. The instrument acts as both transmitter and receiver by bouncing short pulses (pings) of acoustic energy off small particles, plankton and air bubbles. The frequency of the backscattered signals are Doppler shifted proportionally to the average radial (alongbeam) relative velocity between the scatterers and the transducers. Four beams are simultaneously pinged by transducers with a 25°-slant angle in the RDCP-600, and three velocity components are calculated from the backscattered signals.

The self-contained RDCP-600 was deployed to the seabed by divers at the location of 59.561°N, 26.672°E, about 1.5 km offshore. The instrument was deployed for the period between 10 August and 14 September 2006; and, altogether 837.17 hours of multi-layer data were obtained. The mooring depth was about 12 m. Allowing for a 2 m 'blind' distance between the instrument and the lowest measurable cell, plus 2–3 metres at the surface, where measurements are 'contaminated' by wave motion, data from six depth layers were obtained. As a 2 m cell size with 50% overlap was used, '3 m depth' actually means a 2–4 m depth interval, etc. Thus, the data from two adjacent cells are technically somewhat correlated. Each current record included the average value of 300 pings (or individual measurements). A single ping has a statistical noise of 9 cm s^{-1} (2 m cell size, 2 m ping length); the setup we used (300 pings) yielded estimated standard noise levels as low as 0.58 cm s^{-1} for horizontal currents and 0.29 cm s^{-1} for vertical currents.

Apart from measuring currents, the RDCP-600 is equipped with sensors to measure temperature, turbidity and conductivity (i.e. salinity), as well as a highly accurate quartz-based pressure sensor, which measures the depth of the instrument (or relative sea level variations) along with wave parameters such as significant wave height, maximum wave height, peak period, mean period, wave steepness and wave spectrum. These sensors provide only one set of measurements: either in contact with the instrument (temperature, salinity, turbidity) or for the state of the sea surface (sea level, waves). Data output not only includes the above-listed primary time series, but also optional time series of signal strength, standard deviations of each beam, and information about the instrument condition (direction, pitch, roll, battery voltage, etc). The measuring interval was set at 10 min.

The raw data, pre-processed by the special software, was stored on a multi-media card.

In situ measurements also included CTD-soundings and water samplings along the northern coast of Estonia. They were performed during Kunda monitoring cruises and included some stations in the close vicinity of the RDCP mooring site. The surveys took place on 27 May, 27 June, 23 July, 8 August and 14 September 2006. The data from a 20 m deep location (59.557°N, 26.706°E), 0.5 km to the east of the RDCP, was chosen for this study. The CTD-profiles were carried out using either a Seabird-19 probe (for the August survey) or a SAIV-205 probe (for the rest of the surveys). Vertical profiles of water temperature, salinity and fluorescence were measured. At the same time, surface water samples for N_{tot}, P_{tot}, pH, BOD_7 and suspended matter were taken. The samples were analysed in the Pärnu laboratory of the Estonian Marine Institute.

2.3. Satellite images

A good source of environmental satellite images of the Gulf of Finland area for non-commercial purposes is the website of the Finnish Environment Institute (SYKE; URL: http://www.ymparisto.fi). The geoinformatics and land use division of the SYKE produces several remote sensing products, which are based on NOAA AVHRR (NOAA), Terra MODIS (NASA) or ENVISAT MERIS (ESA) satellite observations. The data from environmental satellites are processed and interpreted using special algorithms, and the products for sea surface temperature (SST), algal blooms and sea surface turbidity are presented.

For SST, the Finnish Environment Institute receives 3–4 satellite images daily, but clouds often prevent monitoring at least in some parts of the Baltic Sea. The results are presented as maps, where temperatures are described by colours ranging from blue (colder) to red (warmer). The resolution for the satellite images is 1–2 km depending on the measurement angle. Algal blooms and chlorophyll *a* content is monitored during the summer from June to August using Terra MODIS satellite images received by the Finnish Meteorological Institute. The turbidity is estimated from EOS Terra MODIS images by using an empirically developed algorithm. The Finnish Environment Institute publishes turbidity maps from April to October, but only for the Gulf of Finland.

Our preliminary assortment of images for the period from spring to autumn 2006 yielded a number of very good SST-images, which covered the pre-upwelling, upwelling and post-upwelling conditions. However, the algal bloom and turbidity maps were not so illustrative in this regard.

3. Results and discussion

3.1. Meteorological conditions; variations in sea level and sea surface temperature

The pre-upwelling period in July 2006 passed with a rather normal sequence of small cyclones and anticyclones above Estonia. Air temperatures reached 30°C both in Pakri and Kunda and the seawater was gradually warming up. By the end of July, the water temperature had reached 21°C at both Kunda and Narva Jõesuu and 19–20°C at the other stations along the northern coast of Estonia. As a result of moderate-strength westerlies, an upwelling developed along the southern coast of Hiiumaa Island. Within 2–3 days SST dropped from 17.1°C to 8.4°C at Ristna (Fig. 2b).

From 28 July, northerly winds, and from the evening of 29 July, easterly winds, began to prevail. The Ristna upwelling disappeared by 31 July, but from the same date upwelling evolved in the region of Dirhami. Upwelling does not start immediately after favourable winds have been established. Haapala (1994) has shown that such a wind event must prevail for at least 50 h so that the cumulative wind impulse can reach a certain threshold value. During these 2–3 days, the wind impulse reached a value of about 3500 kg m^{-1} s^{-1} according to the Kunda data and 5000 kg m^{-1} s^{-1} at Pakri, which is quite comparable to the rough estimate of 4000–5000 kg m^{-1} s^{-1} that is required for upwelling according to Haapala (1994). While an impulse of about 5000 kg m^{-1} s^{-1} (50 h of moderate wind) is needed for the creation of upwelling in a stratified coastal sea, a 2–3 times larger impact is needed for a homogeneous sea (Haapala 1994, Alenius et al. 1998). During one and half months the computed total wind impulse reached about 100 000 kg m^{-1} s^{-1}, but more than half of that was associated with westerlies.

The upwelling-favourable easterlies (Fig. 2a) were associated with a large and unusually persistent anticyclone to the east of Estonia. SST dropped rapidly from 17.8°C (on 30 July) to 5.6 degrees (on 1 August) at Dirhami. A few days later the upwelling had spread eastwards as far as Toila (Figs. 2b, 3). Only the somewhat sheltered spot of Narva-Jõesuu remained unaffected.

East winds usually lower the sea level in the eastern section of the Baltic Sea. Indeed, during the upwelling, the sea level was below average (Fig. 4a). When west winds started to prevail on 30 August, the sea level rose by about 1 m according to both tide gauge data and the RDCP.

In regard to prevailing winds and their impact, several sub-periods of the event can be determined. The sub-periods defined primarily by wind statistics are well matched with the temperatures at Dirhami, Pakri and Loksa, but less so with the easternmost stations (Fig. 2). One should also bear in mind the time lag between the beginning of the wind event and
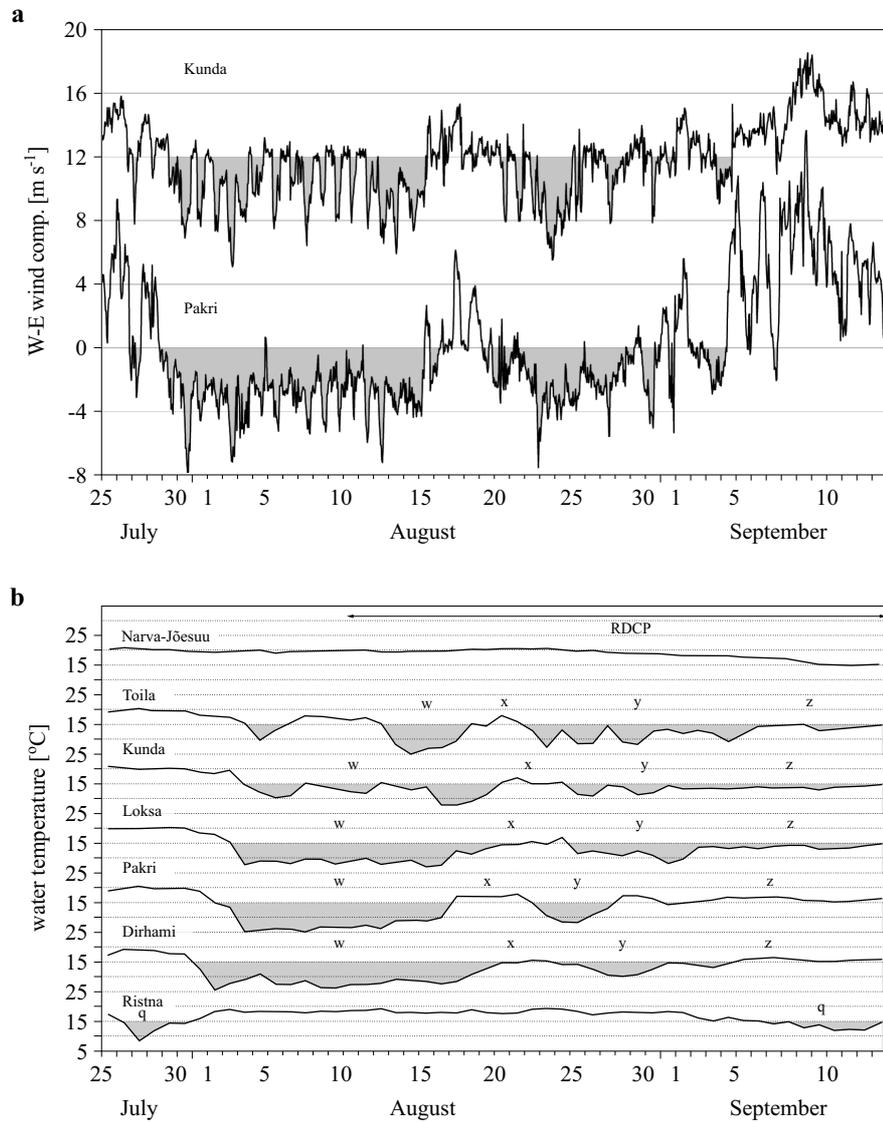
Fig. 2. Variations in the W–E wind component at Kunda and Pakri (a) and water temperature at marine stations along the northern coast of Estonia (see also Fig. 1). The grey areas indicate easterly winds on (a) and temperatures < 15°C on (b). The RDCP deployment period (near Kunda) is marked with an arrow (b); the letters mark the upwelling off the southern coast of Hiiumaa near Ristna (q), the main upwelling (w), relaxation periods (x), resumption of upwelling (y) and post-upwelling warming and mixing (z)

the reaction in water temperature, which reflects the accumulation of the required wind impulse over a certain period. The first upwelling period
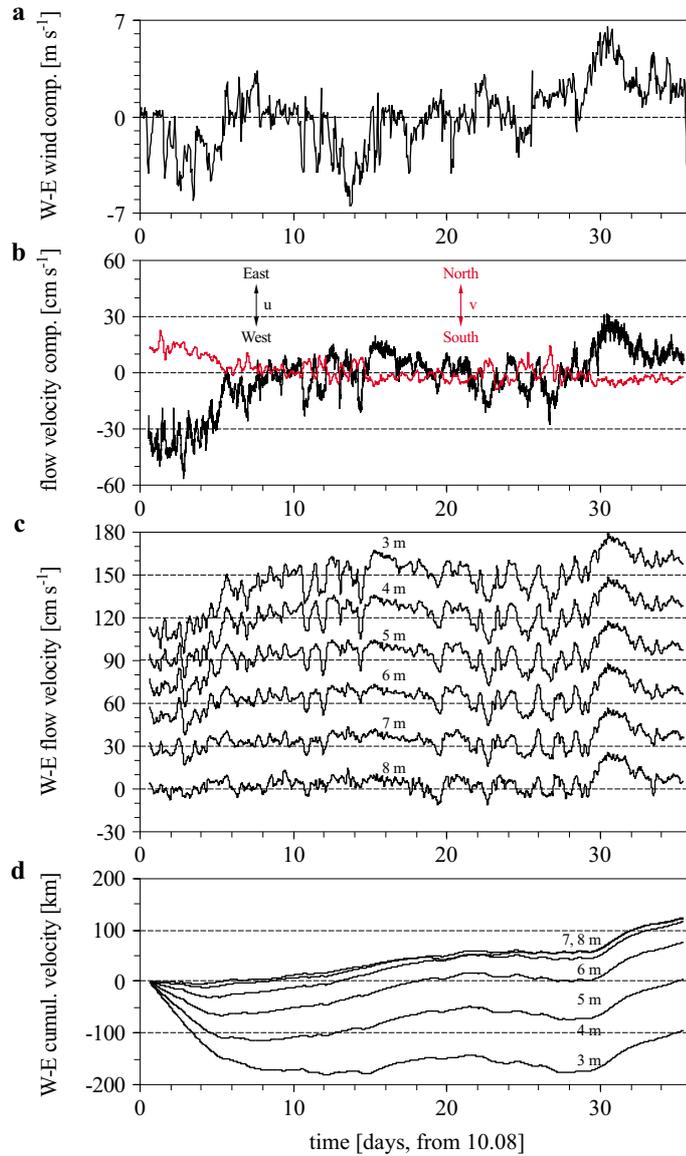
Fig. 3. Hourly average W–E wind speed component at Kunda (a), variations in sub-surface flow components near Kunda (b), vertical structure of W–E flow components (c, offsets of 30 cm s^{-1} are applied to consecutive time series), cumulative graphs of W–E flow velocities in different layers (d) for the period 10 August–14 September 2006. The westerly wind and the corresponding eastward current have a positive direction here

lasted roughly from 30 July to 15 August (Table 1, Fig. 2). Then a short recession associated with westerlies occurred, but by the end of August
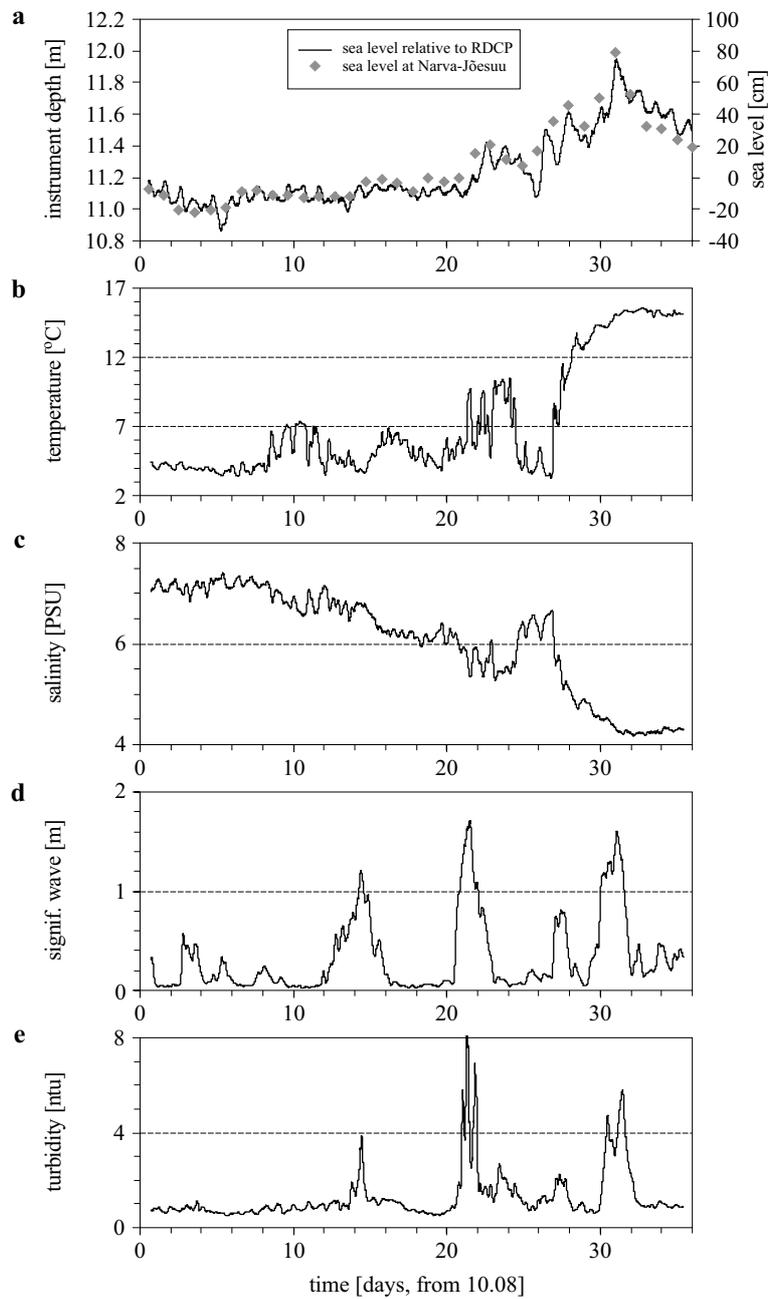
Fig. 4. Relative sea level variations measured as 'instrument depth' together with daily average sea level measurements at the Narva-Jõesuu tide gauge (a), variations in water temperature (b) and salinity (c) at a depth of 11–12 m near Kunda; variations in significant wave heights (d) and near-bottom turbidity (e) at the same location for the period 10 August–14 September 2006

Table 1. Statistics of wind conditions at Kunda and Pakri stations and hydrodynamic data obtained with RDCP during some sub-periods of upwelling (see also Fig. 2a). Note that the hydrodynamic data begin on 10 August

	Date			
	30.07–15.08	16–20.08	21–30.08	31.08–14.09
Period	upwelling	recession	resumption	mixing
Kunda E-wind frequency [%]	76	30	70	17
Pakri E-wind frequency [%]	97	44	90	21
Kunda average wind speed [m s^{-1}]	2.6	2.2	2.8	3.4
Pakri average wind speed [m s^{-1}]	3.2	2.7	3.4	6.0
Kunda max 1 h wind speed [m s^{-1}]	7.8	6.0	6.9	8.3
Pakri max 1 h wind speed [m s^{-1}]	8.0	8.0	9.9	14.2
Kunda max gust wind speed [m s^{-1}]	12.2	13.5	13.5	17.7
Pakri max gust wind speed [m s^{-1}]	13.4	12.5	13.7	25.5
Max sub-surface current [cm s^{-1}]	59.2	28.7	23.3	32.5
Max near-bottom current [cm s^{-1}]	12.7	14.7	17.8	30.0
Max significant wave height [m]	0.6	0.3	1.5	2.0

the upwelling conditions had resumed. The event began to fade due to changing wind conditions between 30 August and 5 September. Strong wave activity (significant wave height up to 2 m, Fig. 4d, Table 1) and vertical mixing during westerly storm winds (gusts up to 25.5 m s^{-1}) dispersed the event by 6 September.

Although the SST data at different coastal stations also depend on their locational features, they still provide a rather telling outline of the event (Fig. 2b). As the coastline bends, small variations in wind direction forced the upwelling zone to swing east- and westwards (Figs. 2, 5). At the coastal marine stations the minimum temperature was as low as 5°C at Toila, 5.4°C at Pakri, 5.6°C at Dirhami, 7°C at Loksa and 8°C at Kunda. The largest temperature drop was observed at Pakri – as much as 15.1°C during 7 days or 14.3°C within 4 days. The temperature of the adjacent water was constantly around 20–21°C, as shown by the data at Narva-Jõesuu (Fig. 2b) and the SST images (Fig. 5).

Altogether 56 nearly daily SST satellite images of the Gulf of Finland were analysed from the period between 10 July and 15 September; only 5 of them were cloud-free and 'perfect'. Twelve revealed about half of the Gulf of Finland area but the other 39 were more or less useless. Fig. 5a presents an example of a good image from the pre-upwelling period. The next two images (Fig. 5b,c) represent the event itself. The temperature on these images ranges from about 6°C to about 21°C. Upwelling along the Estonian coast was detectable on 10 images from the period between 5 and 16 August. The last image (Fig. 5d) shows the post-upwelling mixing
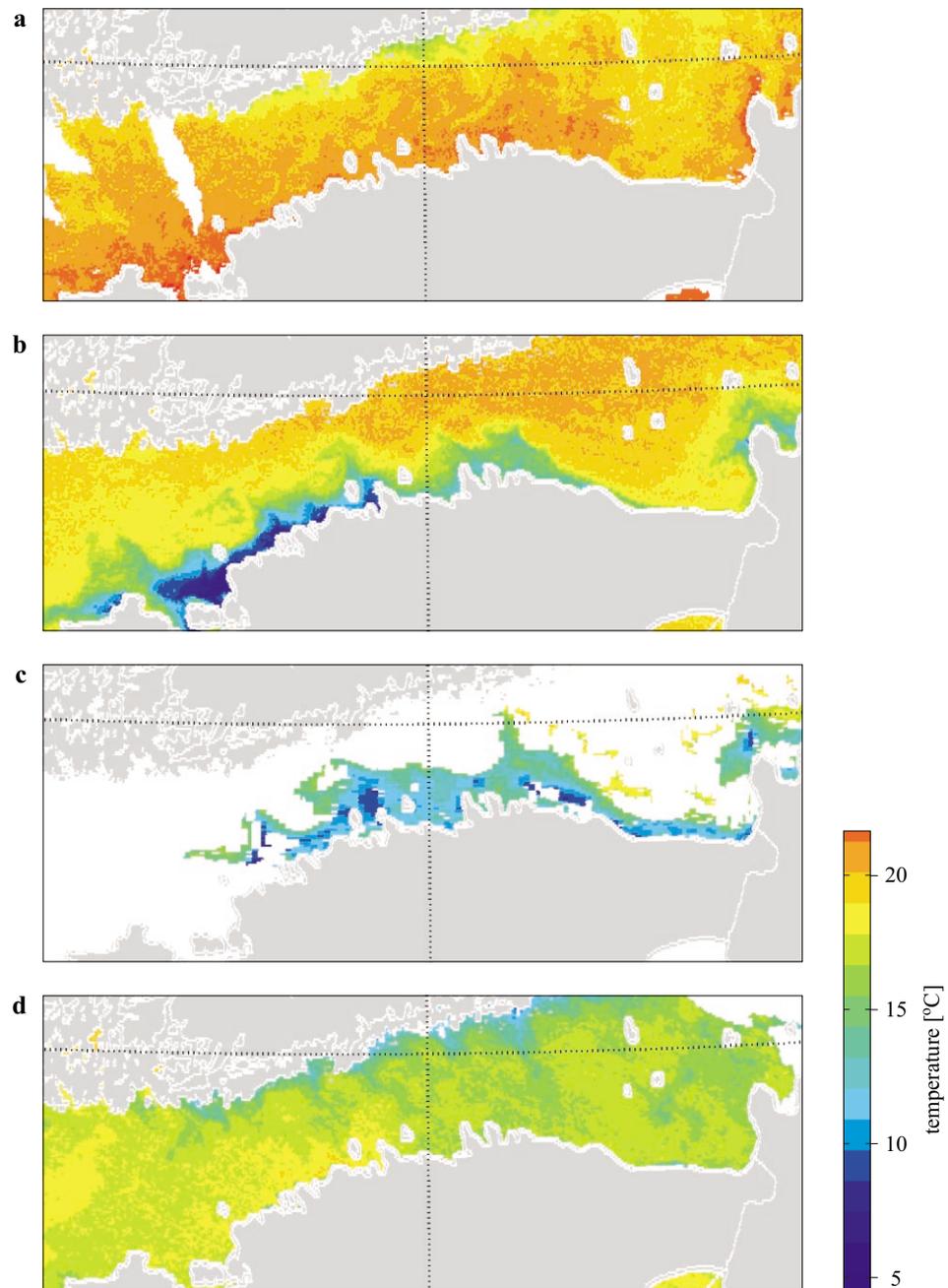
Fig. 5. Sea surface temperature satellite images for the pre-upwelling period (a, 11 July), during the event (b, 7 August; c, 13 August) and the post-upwelling period (d, 13 September). The maximum temperature range within an image (b) is from 6 to 21 degrees. White areas are obscured by clouds

period, when upwelling starts to evolve off the Finnish coast instead. There was no clear evidence of upwelling on the Chl a and turbidity images we analysed, probably because of the low resolution of these images. It is possible, however, that images from some other sources may reveal these features. It also appeared that variations in turbidity were mostly associated with resuspension events during storms (Fig. 4d,e).

According to the SST images, the maximum extension of the event along the Estonian coast reached about 360 km (from the westernmost tip of Hiiumaa Island to Narva-Jõesuu), and probably even more than 400 km, if we add some separate upwelling regions along the Russian coast to the north and east of Narva-Jõesuu (Fig. 5b,c). The images demonstrate, however, that upwelling rarely occurred at its full strength over the whole extension along the north Estonian coast. This is because the coastline bends to the left of the parallel for about 40° in the western part of the coast and to the right for about 20° in the eastern part. Therefore, the zone of the most profound upwelling oscillated east- or westwards depending on the variations in wind direction around the easterly. The cross-shore extension, also measured from the SST images, frequently reached 20–25 km and, taking into account some emerging filaments, even up to 40–45 km. The width of an upwelling is generally determined by the internal (baroclinic) Rossby radius (R1) of the location. According to Alenius et al. (2003) it varies (depending on depth and season) between 1 and 6 km with a median value around 3 km along the Estonian coast of the Gulf of Finland. The zone that is hydrodynamically affected by upwelling (and by its accompanying seaward downwelling zone) does not therefore extend further than about 10 km (e.g. Lehmann et al. 2002). However, during powerful and lasting upwellings, the upwelled water can propagate along the surface much further, as was the case during this particular event.

3.2. Vertical structure of currents

In situ measurement of the vertical structure of horizontal currents during upwelling is quite unique in the Baltic Sea. Due to the proximity to the coast the currents were highly polarised along the axis parallel to the coast. In fact, 68% of all velocity readings and 95% of over 20 cm s^{-1} readings belonged to the two narrow directional intervals of 270–310 and 90–130 degrees. This is also evident from the strong (r = −0.86) correlation between the velocity components u(W–E) and v(S–N) (Fig. 3b). The clearly prevailing W–E velocity component described about 88% of the total variability.

The maximum sub-surface current (59.2 cm s^{-1}) was recorded on 12 August. At the same time, the easterly wind speed was just 5–6 m s^{-1}
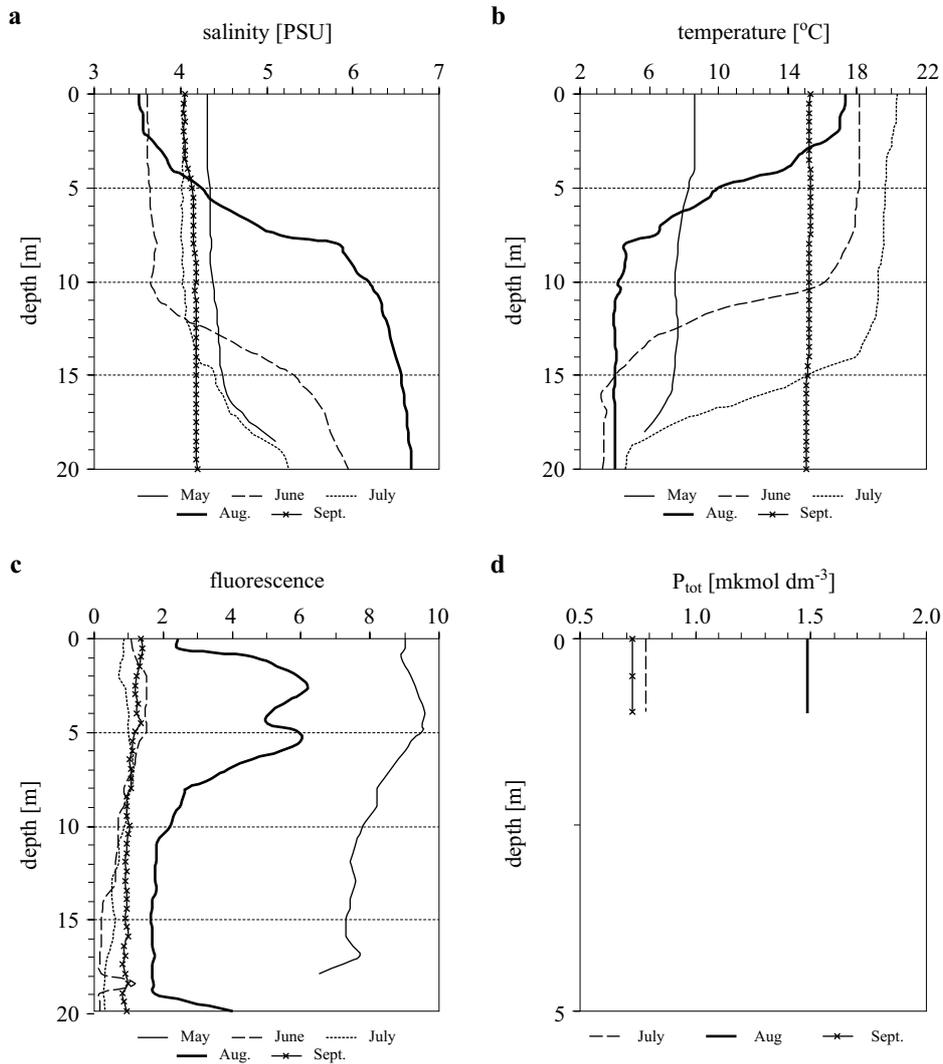
Fig. 6. Vertical profiles of salinity (a), temperature (b) and fluorescence (c), and the averages of three parallel samples of P_{tot} taken from the upper 1 m layer during the three surveys (d) near Kunda. Only the August profiles represent upwelling conditions

at Kunda and 6–8 m s^{-1} at Pakri (Figs. 2a, 3a). The westward flow speed gradually decreased with depth and in the 6–8 m layer the westward current was already negligible ($+10...-15$ cm s^{-1}, Fig. 3c). This difference confirms, firstly, the existence of a pycnocline at a depth of about 7–9 m (see also Fig. 6a,b), and secondly, the existence of a coastal jet. The amazingly large velocities in the upper layer indicate that the upper warmer layer was

effectively blown away and gradually replaced with colder and more saline deep water (Fig. 4b,c). According to theory, the surface Ekman layer divergence affects the sea surface slope in that it causes a geostrophic coastal jet which, in turn, causes a bottom layer response under such circumstances (e.g. Bowden 1983).

It is interesting to mention that, although the 1 h average wind speed reached 8.3 m s^{-1} at Kunda and 14.2 m s^{-1} at Pakri during the stormy days in September (Figs. 2a, 3a, Table 1), the maximum (eastward) current speed was barely 30 cm s^{-1} (Fig. 3c). The current was vertically homogeneous within the measured depth range and the water mass was then vertically mixed for at least 20 m (Fig. 6). It has been shown (e.g. by Weisberg et al. 2000) that upwelling-favourable winds produce disproportionately larger responses in both sea level and currents than downwelling-favourable winds. As the thickness of the upper layer diminishes during an upwelling event, a smaller momentum input at the sea surface is needed, which is also in accordance with the findings of Haapala (1994).

The set of progressive (cumulative) current vectors of different layers illustrate the distinctive relationships between a coastal jet and upwelling. They show the resultant water movement over the period by summing the individual velocity component vectors in such a way that each next vector starts from the end of the previous one. Comparison of the progressive water flow vectors (Fig. 3d) and variations in W–E wind speed component (Figs. 2a, 3a) show that the surface current depended on the local wind, while the near-bottom countercurrent was mostly directed eastwards and against the wind. The curves diverged remarkably during upwelling and continued nearly parallel during the periods of relaxation (Fig. 3d).

RDCP-600 also measures vertical velocities directly. According to both this survey and our experiences in 2003 and 2004 (Suursaar et al. 2005), they were of the order of 1–2 cm s^{-1}. According to the literature, velocities well below 1 mm s^{-1} should be expected in upwelling (e.g. Lehmann et al. 2002, Kowalewski & Ostrowski 2005). In contrast, both Doppler effect-based direct measurements (e.g. Geyer 1993, Wewetzer et al. 1999) and non-hydrostatic 3D models (e.g. Deleersnijder 1989, Kanarska & Maderich 2003) tend to assume much higher vertical velocities. This controversy should be further investigated in the future. In this paper we mistrust the unusually high vertical velocity values, as they did not behave as expected for an upwelling event. We can, however, offer some possible reasons for those high vertical velocity estimates. Firstly, although the calculated velocity components are compensated internally for instrument tilt, the deviation of the instrument from a strictly vertical position may introduce an error. Then, the ratio between the very small 'useful' signal and the relatively

higher noise level has already been pointed out by Suursaar et al. (2005), has the possibility that the particles backscattering RDCP signals might not be neutrally buoyant. The RDCP technology assumes that scatterers flow at the same speed as the water currents. It is possible, however, that a water column contains air bubbles, suspended matter, detritus or small organisms that are not neutrally buoyant, or move up- or downwards for some reason.

3.3. Vertical structure of hydrophysical and hydrochemical variables

Coastal upwelling brings the thermocline to the surface and, as a result, produces a horizontal temperature front (Fig. 5b). Fig. 6 shows vertical profiles of several variables near Kunda obtained just offshore and about 500 m to the east of the RDCP mooring site. Three of them (May, June, July) show a pre-upwelling situation, the one on 8 August represents the upwelling event, and one (in September) describes the vertically homogeneous post-event state. Although at the very moment of CTD-profiling on 8 August the thermocline did not reach the surface (Figs. 5c, 6b), it was nonetheless in a rather elevated position. The position of the halocline (Fig. 6a) was high as well, and high P_{tot} values (Fig. 6d) indicated an input of nutrient-rich water from the deep layers of the Gulf of Finland. There were no significant differences in N_{tot} and BOD_7 values, however. Fluorescence values were not as high as in spring, but still remarkably high (Fig. 6c) for the summer season, when the surface layers are usually depleted of nutrients.

Upwelling-related variations in the near-bottom (11–12 m) temperature ranged between 3.3°C and 15.6°C (Fig. 4b) near Kunda, while the salinity varied between 4.0 and 7.6 PSU (Fig. 4c). During relaxation, the largest increases in temperature were 4.2 degrees in 10 minutes, 6.8°C in 2 hours and 8.3°C in 14 hours. The most rapid salinity drops included 1.5 PSU in 1.5 hours.

3.4. Possible influence on ecological conditions

Upwelling significantly altered the abiotic conditions of the study area, as it was a large and extensive event, and because it was opposed to both the statistical mean circulation features (Alenius et al. 1998, Myrberg & Andrejev 2003, Andrejev et al. 2004) and the hydrological norms for the summer. The hydrobiological implications can be quite complex and they definitely deserve further study on the basis of other data sets.

It usually takes some time before biotic changes are triggered. Vahtera et al. (2005) have shown how late-summer upwelling in the northern coastal

waters of the Gulf of Finland caused above all a decline in phytoplankton biomass and depth-integrated primary production, probably due to growth inhibition by the low temperatures. A bloom-forming cyanobacteria biomass response occurred with a time lag of about 2 to 3 weeks after the upwelling had subsided. Other organisms could benefit from upwelling with an even longer delay. A possible immediate decrease in Chl a and productivity is also discussed by Kręzel et al. (2005b). The depth of a location and the difference between the properties of the upwelled water patch and background values of the adjacent water become important.

Horizontally, the influence of upwelling is not limited strictly to the region of recordable vertical velocities. Offshore widening of the upwelling zone and the development of filaments (Fig. 5b) spread cold, more saline and more nutrient-rich water up to the central part of the Gulf of Finland. Part of this water can occasionally produce a tongue-like inflow into the Väinameri Sea (Fig. 5c). When the wind backed northerly following upwelling-favourable conditions, a southward flow of water began in this system of four straits with a water volume of about 10 km^3 .

Although no noteworthy local upwelling events have occurred in the shallow Väinameri Sea, the whole sub-basin can be filled with water upwelled in the entrance region of the Gulf of Finland. The pronounced changes in ecological conditions resulting from the alternation between upwelled water and water from the Gulf of Riga is described by Astok et al. (1999). However, the mediated influence of upwelling differed from the direct influence, which is evident in the Gulf of Finland: for example, as the trophicity of the Gulf of Riga is considerably higher than in the Baltic Proper, the nutrient concentration of an advected water mass of upwelling origin was lower.

4. Conclusions

On August 2006 a large upwelling occurred along the southern coast of the Gulf of Finland, where downwelling conditions are climatologically more usual. Owing to persistent anticyclonic weather patterns, continuous 5–6 m s^{-1} east winds formed a coastal jet with a near-surface velocity of up to 60 cm s^{-1}, an associated elevation of the thermo- and halocline, and an upflow of cold, saline and more phosphorus-rich water. The complex of hydrophysical and hydrodynamic parameters was registered using an RDCP-600 current profiler moored near Kunda between 10 August and 14 September. According to our analysis of the field data and satellite images, the event can be regarded as a remarkably extensive and strong upwelling. Together with short recession periods, it lasted for about a month. Its longshore extension was about 360 km and its cross-shore extent reached

25 km, filaments excluded. According to data from coastal marine stations, the sea surface temperature dropped from about 21°C to 5°C. On the RDCP mooring site the upwelling-related temperature variations in the near-bottom (11–12 m) layer ranged between 3.3°C and 15.6°C and the salinity varied between 4.0 and 7.6 PSU. CTD profiling showed a rise in both thermo- and halocline and higher fluorescence values during the event. The upwelling conditions were dispersed in the course of westerly storms and high waves at the beginning of September. The effect of the event may be quite complex and far-reaching, but it deserves further study on the basis of other data sets.

Acknowledgements

References

Alenius P., Myrberg K., Nekrasov A., 1998, *The physical oceanography of the Gulf of Finland: a review*, Boreal Environ. Res., 3 (2), 97–125.

Alenius P., Nekrasov A., Myrberg K., 2003, *Variability of the baroclinic Rossby radius in the Gulf of Finland*, Cont. Shelf Res., 23 (6), 563–573.

Andrejev O., Myrberg K., Alenius P., Lundberg P., 2004, *Mean circulation and water exchange in the Gulf of Finland – a study based on three-dimensional modelling*, Boreal Environ. Res., 9 (1), 1–16.

Astok V., Otsmann M., Suursaar Ü., 1999, *Water exchange as the main physical process in semi-enclosed marine systems: the Gulf of Riga case*, Hydrobiologia, 393 (1), 11–18.

Bowden K. F., 1983, *Physical oceanography of coastal water*, Ellis Horwood Ltd., Chichester, 302 pp.

Bychkova I. A., Viktorov S. V., 1987, *Use of satellite data for identification and classification of upwelling in the Baltic Sea*, Oceanology, 27 (2), 158–162.

Deleersnijder E., 1989, *Upwelling and upsloping in three-dimensional marine models*, Appl. Math. Model., 13, 462–467.

Ennet P., Kuosa H., Tamsalu R., 2000, *The influence of upwelling and entrainment on the algal bloom in the Baltic Sea*, J. Marine Syst., 25 (3), 359–367.

Geyer W. R., 1993, *Three-dimensional tidal flow around headlands*, J. Geophys. Res., 98 (C1), 955–966.

Gidhagen L., 1987, *Coastal upwelling in the Baltic Sea: satellite and in situ measurements of sea-surface temperature indicating coastal upwelling*, Estuar. Coast. Shelf Sci., 24 (4), 449–462.

Gill A. E., Clarke A. J., 1974, *Wind-induced upwelling, coastal currents and sea-level changes*, Deep-Sea Res., 21, 325–345.

Haapala J., 1994, *Upwelling and its influence on nutrient concentration in the coastal area of the Hanko Peninsula, entrance of the Gulf of Finland*, Estuar. Coast. Shelf Sci., 38 (5), 507–521.

Jankowski A., 2002, *Variability of coastal water hydrodynamics in the southern Baltic – hindcast modelling of an upwelling event along the Polish coast*, Oceanologia, 44 (4), 395–418.

Kanarska Y., Maderich V., 2003, *A non-hydrostatic numerical model for calculating free-surface stratified flows*, Ocean Dynam., 53 (3), 176–185.

Kowalewski M., Ostrowski M., 2005, *Coastal up- and downwelling in the southern Baltic*, Oceanologia, 47 (4), 453–475.

Krężel A., Ostrowski M., Szymelfenig M., 2005a, *Sea surface distribution during upwelling along the Polish coast*, Oceanologia, 47 (4), 415–432.

Krężel A., Szymanek L., Kozłowski Ł., Szymelfenig M., 2005b, *Influence of coastal upwelling on chlorophyll a concentration in the surface water along the Polish coast of the Baltic Sea*, Oceanologia, 47 (4), 433–452.

Lass H.-U., Schmidt T., Seifert T., 1994, *On the dynamics of upwelling observed at the Darss Sill*, Proc. 19th Conf. Baltic Oceanogr., Gdańsk, 247–260.

Lehmann A., Krauss W., Hinrichsen H.-H., 2002, *Effects of remote and local atmospheric forcing on circulation and upwelling in the Baltic Sea*, Tellus A, 54 (3), 299–316.

Marmorino G. O., Trump C. L., 1992, *Acoustic Doppler current profiler measurements of possible lee waves south of Key West, Florida*, J. Geophys. Res., 97 (C5), 7271–7275.

Myrberg K., Andrejev O., 2003, *Main upwelling regions in the Baltic Sea – a statistical analysis based on three-dimensional modelling*, Boreal Environ. Res., 8 (2), 97–112.

Nõmmann S., Sildam J., Nõges T., Kahru M., 1991, *Plankton distribution during a coastal upwelling event off Hiiumaa, Baltic Sea: impact of short-term flow field variability*, Cont. Shelf Res., 11 (1), 95–108.

Suursaar Ü., Kullas T., 2006, *Influence of wind climate changes on the mean sea level and current regime in the coastal waters of west Estonia, Baltic Sea*, Oceanologia, 48 (3), 361–383.

Suursaar Ü., Kullas T., Otsmann M., 2005, *Vertical structure of horizontal currents and vertical velocities observed off the Estonian coast using a Recording Doppler Current Profiler*, Proc. Estonian Acad. Sci., Biol. Ecol., 54 (3), 190–209.

Vahtera E., Laanemets J., Pavelson J., Huttunen M., Kononen K., 2005, *Effect of upwelling on the pelagic environment and bloom-forming cyanobacteria in the western Gulf of Finland, Baltic Sea*, J. Marine Syst., 58 (1–2), 67–82.

Walin G., 1972, *Some observations of temperature fluctuations in the coastal region of the Baltic*, Tellus, 24, 187–198.

Weisberg R. H., Black B. D., Li Z., 2000, *An upwelling case study on Florida's west coast*, J. Geophys. Res., 105 (C5), 11459–11469.

Wewetzer S. F. K., Duck R. W., Anderson J., 1999, *Acoustic Doppler current profiler measurements in coastal and estuarine environments: examples from the Tay Estuary, Scotland*, Geomorphology, 29 (1), 21–30.

Yanagi T., Ishikawa K., Susami S., 1995, *Convergence, divergence and vertical velocity at a tidal front in Hiuchi-Nada*, J. Oceanogr., 51, 225–238.